Inorganic Chemistry
Article

Inorg. Chem. **2009**, *48*, 11889–11895 **11889**
DOI: 10.1021/ic901965b

Oxidation Chemistry of Axially Protected Mo_2 and W_2 Quadruply Bonded Compounds

Michael Nippe, Eric Victor, and John F. Berry*

Department of Chemistry, University of Wisconsin—Madison, 1101 University Ave. Madison, Wisconsin 53706

Received October 5, 2009

Reported is a facile, high-yielding one-pot synthesis of the quadruply bonded ditungsten (II,II) compound $W_2(dpa)_4$ (**1**) (dpa=2,2′-dipyridylamide), which was obtained from $W(CO)_6$ at high temperature in naphthalene. A similar reaction in 1,2-dichlorobenzene furnished a ditungsten (III, III) species as the major product that was crystallized as $[W_2(dpa)_3Cl_2][BPh_4]$ (**3**). The $[W_2(dpa)_3Cl_2]^+$ cation is better prepared by oxidation of **1** with SO_2Cl_2. Compound **1** was characterized by X-ray crystallography and cyclic-voltammetry, and is compared with its earlier reported molybdenum analogue, $Mo_2(dpa)_4$ (**2**). One-electron oxidation products of **1** and **2**, $[W_2(dpa)_4][BPh_4]$ (**1BPh$_4$**) and $[Mo_2(dpa)_4][BPh_4]$ (**2BPh$_4$**), respectively, have also been synthesized. The crystallographically determined metal−metal distances of 2.23 Å and 2.14 Å in **1BPh$_4$** and **2BPh$_4$**, respectively, are in agreement with metal−metal bond orders of 3.5. Unlike most previously reported Mo_2^{5+} and W_2^{5+} compounds, the primary coordination spheres around the M_2-units in **1**/**1BPh$_4$** and **2**/**2BPh$_4$** remain unchanged upon one-electron oxidation, because the tridentate dpa ligand hinders axial coordination of exogenous ligands.

Introduction

Combination of eight d-electrons from two divalent group VI transition metal ions (Cr^{2+}, Mo^{2+}, W^{2+}) (d^4) can result in the formation of metal−metal quadruple bonds, involving one σ-, two π-, and one δ-bond.[1] These electron rich binuclear M_2^{4+} units, which are of general interest because of their unique electronic and optical properties,[2] advance our understanding of bonding since their oxidation removes electrons from the metal−metal bonding orbitals, resulting in longer M−M distances and lower formal bond orders. The types of chelating ligands currently utilized in quadruply bonded compounds range from O,O donors such as carboxylates[3] to N,O donors such as hydroxypyridinates[4] to N,N donors.[5] Compounds containing a W_2^{4+} unit are less numerous than their Mo_2^{4+} counterparts.[6] Two factors account for the relative scarcity of W_2^{4+} compounds: (1) a more involved synthetic procedure is necessary for the synthesis of W_2^{4+} compounds, and (2) W_2^{4+} compounds are extraordinarily air-sensitive. For example, the generation of binuclear systems employing (N,N) donor-ligands is significantly easier for Mo than for W: $Mo_2(N,N)_4$ species are immediately accessible either by a direct reaction of commercially available $Mo(CO)_6$,[7] or by a ligand substitution reaction of the easily prepared $Mo_2(OAc)_4$ and the desired ligand.[8] The preparation of an analogous $W_2(N,N)_4$ compound typically involves a series of steps starting from comproportionation of $W(CO)_6$ and WCl_6 to produce WCl_4, which is further reduced by an electron-donor such as $NaHBEt_3$ and subsequently reacted with a ligand salt to produce the quadruply bonded target $W_2(N,N)_4$.[9] Even though one-pot reactions between $W(CO)_6$ and hydroxy-pyridines in high-boiling solvents (diglyme) at elevated temperatures have been shown to produce $W_2(N,O)_4$ species,[10−12] the analogous reactions with (N,N)-ligands, such as formamidines, yield either incomplete substituted species (e.g., $W_2(N,N)_4(CO)_2$) or furnish compounds with only triply bonded W_2^{6+} cores.[6] These

*To whom correspondence should be addressed. E-mail: berry@chem.wisc.edu.

(1) Cotton, F. A. In *Multiple Bonds between Metal Atoms*, 3rd ed.; Cotton, F. A., Murillo, C. A., Walton, R. A:, Eds.; Springer Science and Business Media, Inc: New York, 2005.
(2) Alberding, B. G.; Chisholm, M. H.; Chou, Y.-H.; Gallucci, J. C.; Ghosh, Y.; Gustafson, T. L.; Patmore, N. J.; Reed, C. R.; Turro, C. *Inorg. Chem.* **2009**, *48*, 4394–4399.
(3) Chisholm, M. H. *Dalton Trans.* **2003**, 3821–3828.
(4) Brown, D. J.; Chisholm, M. H.; Gribble, C. W. *Dalton Trans.* **2007**, 1793–1801.
(5) Cotton, F. A.; Feng, X.; Matusz, M. *Inorg. Chem.* **1989**, *28*, 594–601.
(6) Cotton, F. A.; Donahue, J. P.; Hall, M. B.; Murillo, C. A.; Villagrán, D. *Inorg. Chem.* **2004**, *43*, 6954–6964.
(7) Lin, C.; Protasiewicz, J. D.; Smith, E. T.; Ren, T. *Inorg. Chem.* **1996**, *35*, 6422–6428.
(8) Holste, G. *Z. Anorg. Allg. Chem.* **1972**, *391*(3), 263–270.
(9) Eglin, J. L. In *Multiple Bonds between Metal Atoms*, 3rd ed.; Cotton, F. A., Murillo, C. A., Walton, R. A:, Eds.; Springer Science and Business Media, Inc: New York, 2005.
(10) Cotton, F. A.; Ilsley, W. H.; Kaim, W. *Inorg. Chem.* **1980**, *19*, 1450–1452.
(11) Cotton, F. A.; Niswander, R. H.; Sekutowski, J. C. *Inorg. Chem.* **1978**, *17*, 3541–3545.
(12) Cotton, F. A.; Niswander, R. H.; Sekutowski, J. C. *Inorg. Chem.* **1979**, *18*, 1152–1159.

Published on Web 11/18/2009

reactions are further complicated by the inferior thermal stability of formamidines, which prevents the use of high reaction temperatures that are necessary for the removal of carbonyl ligands from tungsten.

We report here the first direct one pot synthesis of a binuclear quadruply bonded W(II) compound with (N,N)-donor ligands, $W_2(dpa)_4$ (**1**) (dpa = 2,2′-dipyridylamide) starting from commercially available $W(CO)_6$ and dpaH in refluxing naphthalene. Compound **1** is of interest to us as a precursor for new heterotrimetallic complexes.[13−15]

Here the redox chemistry of **1** and the analogous dimolybdenum compound $Mo_2(dpa)_4$ (**2**)[16] is investigated. Interestingly, the axial positions in **1** and **2** are well protected by coordination of the pendant pyridine groups of the dpa (vide infra), which prohibits the binding of exogenous ligands. By retaining the primary coordination sphere of the M_2^{4+} and M_2^{5+} units we can accurately analyze the geometric changes caused by removal of one electron from the δ-manifold of **1** and **2**.

Experimental Section

Materials and Methods. All reactions were carried out under a dry N_2 atmosphere using Schlenk techniques and glovebox methods. Solvents diethyl ether (Et_2O), tetrahydrofuran (THF), and hexanes were purified using a Vacuum Atmospheres solvent purification system. Dichloromethane was freshly distilled under an N_2 atmosphere over CaH_2 prior to use. $W(CO)_6$ (STREM), naphthalene (Sigma-Aldrich), 1,2-dichlorobenzene (Sigma-Aldrich) tetrabutylammonium hexafluorophosphate ([NBu_4][PF_6]), tetrabutylammonium tetraphenylborate ([NBu_4][BPh_4], Sigma-Aldrich), SO_2Cl_2 (1 M in CH_2Cl_2 from Sigma-Aldrich), and I_2 (Sigma-Aldrich) were purchased and used as received. The ligand dpaH (2,2′-dipyridylamine, Sigma-Aldrich) was recrystallized from hot hexanes prior to use. $Mo_2(dpa)_4$ (**2**) was prepared according to a literature procedure.[15] Cyclic voltammograms (CVs) were taken on a BAS Epsilon-EC instrument using CH_2Cl_2 solutions with 0.1 M NBu_4PF_6 and < 1 mM substrate. The electrodes were as follows: glassy carbon (working), Pt wire (auxiliary), and Ag/AgCl in CH_3CN (reference). The potentials were referenced versus the ferrocene/ferrocenium redox couple, by externally added ferrocene. Elemental analysis was carried out by Columbia Analytical Services (formerly Desert Analytics) in Arizona, U.S.A. Mass spectrometry data were recorded at the Mass Spectrometry Facility of the Chemistry Instrument Center of the University of Wisconsin-Madison. Matrix-assisted laser desorption/ionization (MALDI) mass spectra were obtained using a Bruker REFLEX II (Billerica, MA) equipped with a 337 nm laser, a reflectron, delayed extraction, and a time-of-flight (TOF) analyzer. In the positive ion mode, the acceleration voltage was 25 kV. EPR spectra were recorded at room temperature on CH_2Cl_2 solutions using a Bruker EleXsys EPR: E-500-A console with ER 049SX SuperX Bridge and SuperX Cavity. The parameters were as follows for **1BPh$_4$**/**2BPh$_4$**: microwave frequency = 9.834548/9.836937 GHz, microwave power = 0.6325 mW, center Field = 3772/3599 G, sweep width = 600 G, modulation amplitude = 1 G, modulation frequency = 3 kHz, time constant = 1.28 ms. The IR spectra were taken on a BRUKER TENSOR 27 using KBr techniques. The UV−vis spectra were recorded under an atmosphere of N_2 on a VARIAN CARY 50 Scan UV−visible Spectrophotometer using quartz cells (path length 1.00 cm). ^{1}H NMR spectra were recorded on a Bruker AC+ 300 NMR spectrometer.

X-ray Structure Determinations. $W_2(dpa)_4$ (1). A purple needle-shaped crystal of **1** with approximate dimensions 0.04 × 0.02 × 0.02 mm was selected under oil under ambient conditions and attached to the tip of a MiTeGen MicroMount. The crystal was mounted in a stream of cold nitrogen at 100(2) K and centered in the X-ray beam of a Bruker SMART APEXII diffractometer with Cu Kα (λ = 1.54178 Å) radiation. The initial cell constants were determined through an auto-indexing routine built into the APEXII program, but were also read into CELLNOW. The crystal was found to be a two-component twin with domains related to each other by a 180° rotation around the *b* axis. A full sphere of data was collected to a resolution of 0.82 Å. Using the TWINABS routine an HKLF4 file was created using reflections from both domains. The structure was solved using the Patterson method and refined by least-squares refinement on F^2 followed by difference Fourier synthesis. All hydrogen atoms were included in the final structure factor calculation at idealized positions and were allowed to ride on the neighboring atoms with relative isotropic displacement coefficients. The metal atoms occupy positions along a crystallographic 2-fold axis. Using the HKLF5 file for all reflections and refining the batch scale factor (final value 0.42) decreased the R_1 further (Table 1).

[$W_2(dpa)_4$][BPh_4] (1BPh$_4$), [$Mo_2(dpa)_4$][BPh_4] (2BPh$_4$), and [$W_2(dpa)_3Cl_2$][BPh_4] (3). Crystals were selected under oil under ambient conditions and block-(**1BPh$_4$** and **2BPh$_4$**) or needle-(**3**) shaped single crystals were attached to the tip of a nylon loop. The crystals were mounted in a stream of cold nitrogen at 100(2) K and centered in the X-ray beam of a Bruker CCD-1000 diffractometer (Mo Kα) using a video camera. The data were successfully indexed by an auto-indexing routine built into the SMART program.[18] The structures were solved using direct methods and refined by least-squares refinement on F^2 followed by difference Fourier synthesis. All hydrogen atoms were included in the final structure factor calculation at idealized positions and were allowed to ride on the neighboring atoms with relative isotropic displacement coefficients.

$W_2(dpa)_4$ (1). $W(CO)_6$ (1.03 g, 2.92 mmol) and dpaH (1.00 g, 5.84 mmol) were combined at room temperature with naphthalene (5 g). The flask was placed into a preheated sandbath (250 °C) and stirred for 2 h. Successive color changes from colorless to yellow, orange, red, purple brown, and finally blue were observed. The solution was allowed to cool down to room temperature, and the resulting solid was subsequently washed with hot hexanes (2 × 50 mL, 1 × 30 mL) and CH_2Cl_2 (20 mL). The remaining blue crystalline solid was then kept at 90 °C under vacuum for 1 h. Yield: 1.21 g (79%). Anal. Calcd for $C_{40}H_{32}W_2N_{12}$ (**1**): C, 45.82%; H, 3.08%; N, 16.03%. Found: C, 45.74%; H, 3.15%; N, 15.86%. MALDI-Mass spectrum (100% peak): m/z = 1047.8 [**1**]$^+$. ^{1}H NMR (CD_2Cl_2, ppm): 8.16−8.15 (m, 4 H), 7.53−7.49 (m, 8 H), 6.79−6.77 (m, 4 H). IR (KBr, cm^{-1}): 2360 m, 2341 m, 1596 s, 1523 m, 1458 s, 1438 s, 1363 w, 1340 w, 1313 w, 1278 w, 1242 w, 1149 m, 1016 w, 991 w, 952 w, 910 w, 769 m, 734 w.

X-ray qualtity crystals of **1** were obtained by heating 500 mg of **1** in naphthalene (4 g) to 200 °C for 15 min in a 100 mL Schlenk flask. The resulting dark blue solution was slowly cooled and kept at 130 °C for 10 h after which small needle shaped crystals, suitable for X-ray crystallography, had formed.

[$W_2(dpa)_4$][BPh_4] (1BPh$_4$). CH_2Cl_2 (45 mL) was added to a mixture of blue **1** (300 mg, 0.29 mmol) and I_2 (36 mg, 0.14 mmol) at room temperature, and the dark purple mixture was stirred for 40 min. The purple mixture was filtered into a flask containing dried [NBu_4][BPh_4] (163 mg, 0.29 mmol), and the filtrate was

(13) Nippe, M.; Berry, J. F. *J. Am. Chem. Soc.* **2007**, *129*, 12684–12685.
(14) Nippe, M.; Timmer, G. H.; Berry, J. F. *Chem. Commun.* **2009**, 4357–4359.
(15) Nippe, M.; Victor, E.; Berry, J. F. *Eur. J. Inorg. Chem.* **2008**, 5569–5572.
(16) Suen, M. C.; Wu, Y.; Chen, J. D.; Keng, T. C.; Wang, J. C. *Inorg. Chim. Acta* **1999**, *288*, 82–89.
(17) Schubert, E. M. *J. Chem. Educ.* **1992**, *69*, 62–64.
(18) *SADABS V.2.05, SAINT V.6.22, SHELXTL V.6.10 & SMART 5.622*; Bruker-AXS: Madison, WI, 2000−2003.

Table 1. Crystallographic Data

compound	**1**	**1BPh$_4$** (CH_2Cl_2/hexanes)	**1BPh$_4$** (CH_2Cl_2/Et_2O)	**2 BPh$_4$** (CH_2Cl_2/hexanes)	**2 BPh$_4$** (CH_2Cl_2/Et_2O)	**3·2CH$_2$Cl$_2$**
formula	$W_2(dpa)_4$	$W_2(dpa)_4(B(C_6H_5)_4)$	$W_2(dpa)_4(B(C_6H_5)_4)$	$Mo_2(dpa)_4(B(C_6H_5)_4)$	$Mo_2(dpa)_4(B(C_6H_5)_4)$	$W_2(dpa)_3Cl_2(B(C_6H_5)_4)\cdot 2CH_2Cl_2$
crystal system	monoclinic	monoclinic	monoclinic	monoclinic	monoclinic	triclinic
space group	$C2/c$	$C2/c$	$P2_1$	$C2/c$	$P2_1$	$P\bar{1}$
a, Å	18.1386(7)	20.648(4)	8.9775(7)	20.596(2)	8.9852(6)	12.892(2)
b, Å	11.5046(4)	18.568(4)	27.614(2)	18.554(2)	27.653(2)	13.561(2)
c, Å	16.6777(6)	16.291(3)	10.7148(8)	16.288(2)	10.6952(8)	16.281(2)
α, deg						95.344(3)
β, deg	101.348(3)	122.096(3)	90.388(2)	122.106(1)	90.401(1)	97.282(3)
γ, deg						106.848(3)
V, Å^3	3412.2(2)	5219.3	2656.2(4)	5272.5(10)	2657.3(3)	2676.9(7)
Z	4	4	2	4	2	2
ρ, Mg m^{-3}	2.041	1.717	1.710	1.501	1.490	1.784
R1[a], wR2[b] ($I < 2\sigma(I)$)	0.0362, 0.0829	0.0244, 0.0608	0.0205, 0.0530	0.0288, 0.0690	0.0219, 0.0580	0.0372, 0.0957
R1[a], wR2[b] (all data)	0.0551, 0.0913	0.0321, 0.0727	0.0213, 0.0562	0.0383, 0.0752	0.0233, 0.0638	0.0549, 0.1136

[a] $R1 = \sum||F_o| - |F_c||/\sum|F_o|$. [b] $wR2 = [\sum w(F_o^2 - F_c^2)^2/\sum w(F_o^2)^2]^{1/2}$, $w = 1/\sigma^2(F_o^2) + (aP)^2 + bP$, where $P = [\max(0 \text{ or } F_o^2) + 2(F_c^2)]/3$.

subsequently layered with Et_2O. Crystals of **1BPh$_4$** ($P2_1$) suitable for X-ray crystallography were obtained after 1 day. Layering CH_2Cl_2 solutions of **1BPh$_4$** with hexanes instead of ether resulted in monoclinic crystals with spacegroup $C2/c$.

Yield: 240 mg (61%). Anal. Calcd for $C_{64}H_{52}W_2N_{12}B$ (**1BPh$_4$**): C, 56.20%; H, 3.83%; N, 12.29%. Found: C, 55.37%; H, 3.97%; N, 12.26%. MALDI-Mass spectrum (100% peak): m/z = 1047.7 $[1]^+$. IR (KBr, cm^{-1}): 3051 w, 2997 w, 1600 m, 1581 m, 1456 s, 1431 s, 1369 w, 1305 w, 1280 w, 1228 w, 1151 w, 1018 w, 960 w, 848 w, 773 w, 763 w, 732 w, 703 w, 613 w.

[Mo$_2$(dpa)$_4$][BPh$_4$] (2BPh$_4$). CH_2Cl_2 (45 mL) was added to a mixture of red **2** (300 mg, 0.34 mmol) and I_2 (87 mg, 0.34 mmol) at room temperature, and the resulting dark brown mixture was stirred for 40 min. The brown mixture was filtered into a flask containing dried $[NBu_4][BPh_4]$ (193 mg, 0.34 mmol). This solution was layered with Et_2O, and crystals of **2BPh$_4$** ($P2_1$) suitable for X-ray crystallography were obtained after 1 day. Layering CH_2Cl_2 solutions of **2BPh$_4$** with hexanes instead of ether resulted in monoclinic crystals with spacegroup $C2/c$.

Yield: 250 mg (61%). Anal. Calcd for $C_{64}H_{52}Mo_2N_{12}B$ (**2BPh$_4$**): C, 64.49%; H, 4.40%; N, 14.10%. Found: C, 62.37%; H, 4.29%; N, 13.39%. MALDI-Mass spectrum (100% peak): m/z = 872 $[2]^+$. IR (KBr, cm^{-1}): 3037 w, 2995 w, 2362 w, 2339 w, 1598 m, 1581 m, 1458 s, 1433 s, 1367 w, 1305 w, 1280 w, 1228 w, 1153 w, 1143 w, 1016 w, 846 w, 775 w, 763 w, 732 w, 702 w.

[W$_2$(dpa)$_3$Cl$_2$][BPh$_4$] (3). 1,2-Dichlorobenzene (dcb) (20 mL) was added to $W(CO)_6$ (400 mg, 1.14 mmol) and dpaH (290 mg, 1.71 mmol) in a 100 mL Schlenk flask. The flask was equipped with a water cooled reflux condenser, placed into a preheated sand bath (250 °C), and stirred under heavy reflux for 12 h. The resulting brown mixture was filtered, and the filtrate was dried under reduced pressure. The remaining brown solid was extracted with CH_2Cl_2 (50 mL) and filtered into a flask containing dried $[NBu_4][BPh_4]$ (320 mg, 0.57 mmol). Layering the dark brown solution with Et_2O resulted in the formation of a brown precipitate, that was collected by filtration and recrystallized two times from CH_2Cl_2/Et_2O yielding small amounts of brown needle shaped crystals of **3·2CH$_2$Cl$_2$** and brown precipitate. It was not possible to separate these very fine needles from the precipitate to obtain pure enough samples for elemental analysis. MALDI-Mass spectrum (100% peak): m/z = 915.2 $[W_2(dpa)_3Cl]^+$, 950.2 $[W_2(dpa)_3Cl_2]^+$. ^{1}H NMR (CD_2Cl_2, ppm): 8.41 (d, 2 H), 7.96 (d, 2 H), 7.80 (m, 6 H), 7.45 (d, 4 H), 7.23 (m, 23 H), 7.09−6.88 (m, 30 H), 6.83−6.73 (m 12 H).

[W$_2$(dpa)$_3$X$_2$][BPh]$_4$ (4, X = Cl, I). CH_2Cl_2 (25 mL) was added to solid **1** (210 mg, 0.20 mmol) and I_2 (190 mg, 0.75 mmol), and the greenish-brownish mixture was stirred for 12 h at room temperature. The mixture was filtered into a flask containing dried $[NBu_4][BPh_4]$ (130 mg, 0.23 mmol), and the filtrate was subsequently layered with Et_2O. A few needle shaped crystals were obtained after 2 days.

MALDI-Mass spectrum (100% peak): m/z = 949.8 $[W_2(dpa)_3Cl_2]^+$, 1039.7 $[W_2(dpa)_3ClI]^+$, and 1131.8 $[W_2(dpa)_3I_2]^+$.

[W$_2$(dpa)$_3$Cl$_2$][Cl] (5). The dropwise addition of a 1 M solution of SO_2Cl_2 in CH_2Cl_2 (0.36 mL) to a vigorously stirred blue mixture of $W_2(dpa)_4$ (360 mg, 0.34 mmol) and dried LiCl (120 mg, 2.86 mmol) in CH_2Cl_2 (30 mL) at room temperature caused an initial color change to purple and then to brown. After stirring the mixture for 1 h, tetrahydrofuran (THF, 20 mL) was added, and the mixture was stirred for 10 h. All solvents were removed under reduced pressure, and the resulting brown solid was dried under vacuum. Extraction with CH_2Cl_2 (30 mL) yielded a brown solution that was layered with Et_2O. Crystals of **5·CH$_2$Cl$_2$** were obtained within 3 days. Yield: 140 mg (38%). Anal. Calcd for $C_{31}H_{26}Cl_5N_9W_2$ (**5·CH$_2$Cl$_2$**): C, 34.81%; H, 2.45%; N, 11.79%. Found: C, 34.81%; H, 2.49%; N, 11.19%. MALDI-Mass spectrum (100% peak): m/z = 982.6 $[W_2(dpa)_3Cl_3]^+$, 949.6 $[W_2(dpa)_3Cl_2]^+$, 912.7 $[W_2(dpa)_3Cl]^+$. ^{1}H NMR (CD_2Cl_2, ppm): 8.42 (d, 2 H), 7.98−7.93 (m, 4 H), 7.82 (t, 2 H), 7.63 (d, 2 H), 7.32−7.23 (m, 6 H), 7.14−7.09 (m, 2), 7.02−6.98 (m, 4 H), 6.83 (t, 2 H). IR (KBr, cm^{-1}): 1604 m, 1590 s, 1559 m, 1481 s, 1457 s, 1443 s, 1375 w, 1349 w, 1265 m, 1127 w, 1151 m, 1111 m, 1025 w, 955 w.

Results and Discussion

Synthesis. The synthesis of $W_2(dpa)_4$ (**1**) is efficiently accomplished in the reaction of commercially available $W(CO)_6$ with 2 equiv of dpaH in refluxing naphthalene (reaction a, Scheme 1). A color change to dark blue indicates that the reaction is complete.

The low solubility of **1** in common solvents made its crystallization difficult, but it was possible to obtain crystals suitable for X-ray crystallography by slow cooling of a solution of **1** in naphthalene.

When the reaction of $W(CO)_6$ and dpaH was carried out in refluxing 1,2-dichlorobenzene (reaction b, Scheme 1) instead of naphthalene, the resulting brown mixture contained both **1** and the binuclear cation $[W_2(dpa)_3Cl_2]^+$. These could be separated by filtration to yield a brown solution. Evaporation of the solvent yielded a brown powder that was dissolved in CH_2Cl_2. Addition of $[NBu_4][BPh_4]$ to this brown solution and slow

Scheme 1. (a) $T \sim 220$ °C; (b) $T \sim 180$ °C; (c) 3 I_2, $[NBu_4][BPh_4]$, 12 h; (d) 0.5 I_2, $[NBu_4][BPh_4]$, 40 min

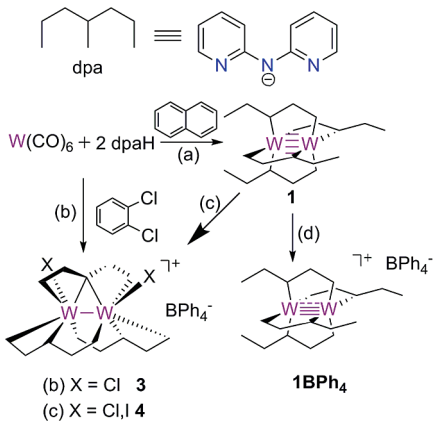

solvent diffusion of Et_2O yielded brown crystals of $[W_2(dpa)_3Cl_2][BPh_4]$ (**3**). There are two possible pathways for the formation of **3** in this reaction: (1) the competitive direct synthesis of **3** over **1** and (2) the oxidation of previously formed **1** and concomitant loss of one dpa ligand to form **3**. To distinguish between these pathways, pure **1** (generated from reaction a) was refluxed in 1,2-dichlorobenzene, and the formation of $[W_2(dpa)_3Cl_2]^+$ was observed by MALDI-TOF MS. We further investigated the two-electron oxidation of **1** by addition of excess I_2 to **1** in CH_2Cl_2 (reaction c). From this reaction mixture a small amount of crystalline material of $[W_2(dpa)_3X_2][BPh_4]$ (**4**) was obtained, in which X is a mixture of Cl^- and I^-. The presence of $[W_2(dpa)_3Cl_2]^+$, $[W_2(dpa)_3ClI]^+$, and $[W_2(dpa)_3I_2]^+$ species in **4** was also verified by mass spectrometry, which strongly suggests the involvement of CH_2Cl_2 as a chloride source. Having established that formation of **3** during reaction (b) involves oxidation of **1**, the use of 1,2-dichlorobenzene as a solvent in the preparation of **1** is disfavored and therefore reaction (a) is the preferred method to cleanly obtain **1**. Our optimized reaction conditions for the preparation of the $[W_2(dpa)_3Cl_2]^+$ cation are as follows: Stoichiometric oxidation of **1** with SO_2Cl_2 in CH_2Cl_2 in the presence of LiCl yielded the desired ditungsten (III, III) species as the chloride salt $[W_2(dpa)_3Cl_2]Cl$ (**5**) in high purity.

Treatment of **1** in CH_2Cl_2 with a stoichiometric amount of iodine furnished a one-electron oxidized species which could be isolated and crystallized as $[W_2(dpa)_4][BPh_4]$ (**1BPh$_4$**). The same procedure was also successful when applied to the molybdenum analogue of **1**, $Mo_2(dpa)_4$ (**2**),[16] furnishing $[Mo_2(dpa)_4][BPh_4]$ (**2BPh$_4$**).

Crystal Structures. The crystal structure of **1** is shown in Figure 1, and relevant bond distances are given in Table 2. Each of the four dpa ligands is bonded via one amido N atom (N_a) and one pyridine N atom (N_{py}(s)) with interestingly equal averaged metal−ligand distances of 2.132[5] Å. Additionally the N atoms of the pendant pyridine rings (N_{py}(l)) are weakly coordinated to the W_2-unit in a manner consistent with the structures of $Cr_2(dpa)_4$,[19] $Mo_2(dpa)_4$,[16] and $WMo(dpa)_4$.[14] In **1**, the

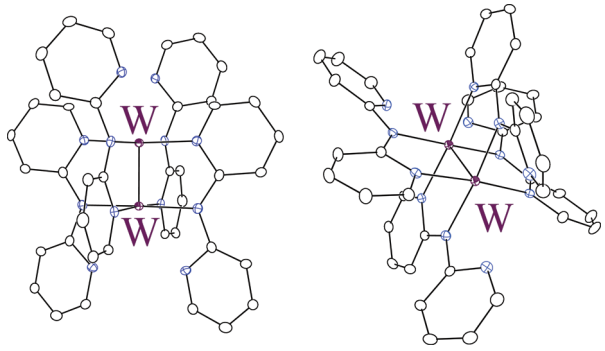

Figure 1. Molecular structures of **1** (left) and the $[W_2(dpa)_4]^+$ cation in **1BPh$_4$** (right) with displacement ellipsoids drawn at the 30% probability level. Hydrogen atoms have been omitted for clarity.

W···N_{py}(l) distances on one end of the molecule are both 2.755(5) Å, while the W···N_{py}(l) distances to the other W atom are 3.109(5) Å. As a possible result of these weak axial interactions, the W≡W bond length is about 0.03 Å longer than in $W_2(hpp)_4$ (hpp = the anion of 1,3,4,6,7,8-hexahydro-2*H*-pyrimido[1,2-*a*]pyrimidine)[20] and in the closely related $W_2(PhNpy)_4$ (PhNpy = 2-anilinopyridinate).[21] The M−N_a and M−N_{py}(s) distances are shorter than in the molybdenum analogue of **1**, $Mo_2(dpa)_4$ (**2**), by ~0.03 and 0.04 Å, respectively (Table 2).

The above-mentioned weak coordination of the pendant pyridine rings to the axial regions of the M_2 unit proffers **1** and **2** as ideal compounds to study structural changes upon oxidation of M_2^{4+} to M_2^{5+} without altering the primary coordination sphere around the metals, as these axial sites are protected against coordination of exogenous ligands. The M−M distances in **1BPh$_4$** and **2BPh$_4$** (Figure 2) are longer than in **1** and **2** by 0.033 and 0.046 Å, respectively, which is consistent with the removal of one electron from the highest metal−metal bonding orbital (δ), resulting in a formal bond order of 3.5. Interestingly, the M−N_a bond lengths decrease upon oxidation by 0.03 and 0.06 Å for W and Mo, whereas the M−N_{py}(s) bonds increase by 0.025 Å for W and do not significantly change in the case of Mo. The most dramatic change, however, is observed for the M···N_{py}(l) distances: The sum of all M···N_{py}(l) distances (Table 3 and 4) is 0.57 Å ($P2_1$)/ 0.62 Å ($C2/c$), and 0.60 Å ($P2_1$)/ 0.70 Å ($C2/c$) shorter in **1BPh$_4$** and **2BPh$_4$**, respectively, than in their quadruply bonded parent complexes. The M···N_{py}(l) shortening could clearly indicate enhanced interactions between the N_{py}(l) atoms and the M_2 units. In detail, the predominant interaction is anticipated to be increased electron donation from the N_{py}(l) lone pair into the metal d_{xz} and d_{yz} orbitals, thereby increasing the population of metal−metal π^* orbitals and elongating the M−M bond length. Quantitative evaluation of this effect can be made using the direction angle, defined by Cotton as the M−N_a−C−N_{py}(l) torsion angle.[19] For small values of the direction angle ($\sum < 20°$), the orientation of N_{py}(l) is optimal to allow for π-type interactions with M_2. The sum of the direction angles in **1** and **2** are 106.8[5]° and 104.2[5]°, respectively, very similar with

(19) (a) Cotton, F. A.; Daniels, L. M.; Murillo, C. A.; Pascual, I.; Zhou, H.-C. *J. Am. Chem. Soc.* **1999**, *121*, 6856–6861. (b) Edema, J. J. H.; Gambarotta, S.; Meetswa, A.; Spek, A. L.; Smeets, W. J. J.; Chiang, M. Y. *J. Chem. Soc., Dalton Trans.* **1993**, 789.

(20) Cotton, F. A.; Huang, P.; Murillo, C. A.; Timmons, D. J. *Inorg. Chem. Commun.* **2002**, *5*, 501–504.

(21) Chakravarty, A. R.; Cotton, F. A.; Shamshoum, E. S. *Inorg. Chem.* **1984**, *23*, 4216–4221.

Table 2. Selected Interatomic Distances in **1**, **2**,[16] **1BPh$_4$**, and **2BPh$_4$**

		1BPh$_4$			**2BPh$_4$**	
	1	*C*2/*c*	*P*2$_1$	**2**	*C*2/*c*	*P*2$_1$
M−M, Å	2.1934(4)	2.2275(5)	2.2259(2)	2.097(2)	2.1423(4)	2.1429(2)
M−N$_{py}$(s), Å	2.132[5]	2.1465[3]	2.157[3]	2.178[4]	2.167[2]	2.176[2]
M−N$_a$(s), Å	2.132[5]	2.102[3]	2.101[3]	2.167[4]	2.114[2]	2.108[2]
M1···N$_{py}$(l), Å	2.775(5)	2.713(3)	2.780(3), 2.797(3)	2.786(5)	2.720(2)	2.808(2), 2.815(2)
M2···N$_{py}$(l), Å	3.109(5)	2.861(3)	2.619(3), 2.998(3)	3.155(4)	2.868(2)	2.630(2), 3.029(2)

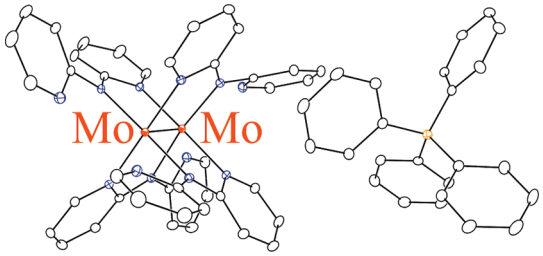

Figure 2. Molecular structure of **2BPh$_4$** with displacement ellipsoids drawn at the 30% probability level. Hydrogen atoms have been omitted for clarity.

those reported for $Cr_2(dpa)_4$ (104[3]°), and indicate rather weak π^* interactions.[19] Upon oxidation, even though all the M···N$_{py}$(l) distances shorten, the direction angles do not change significantly. Therefore, no significant increase in π^* interactions is expected, and the strong decrease in M···N$_{py}$(l) distances may be solely attributed to electrostatic interactions and the decrease of the metal d-orbital radii upon oxidation.

We also investigated the molecular structure of **3** by X-ray crystallography. The W_2^{6+} unit is surrounded by two Cl^- ions and three ligating dpa ligands. Two of the dpa moieties adopt a chelating/bridging binding mode in which one W atom is chelated by one pyridine N atom and the central amide N atom and the other pyridine N atom binds to the second W atom (Figure 3, Table 5). Interestingly, one of the dpa moieties in **3** shows the rare "doubly chelating/bridging"[22] coordination mode[23,24] that has so far never been reported for any metal−metal bonded compound. The molecule has overall C2 symmetry with the C2 axis passing through the central N atom of the doubly chelating/bridging ligand and the midpoint between the two W atoms. The coordination geometry of the W atoms is best described as capped octahedral. The overall charge suggests a formal oxidation state of +3 for both tungsten ions. Additionally, the W−W distance of 2.5310(7) Å is more than 0.30 Å longer than in **1BPh$_4$**, as a result of the lower bond order in **3** as compared to **1** and **1BPh$_4$** and the loss of one chelating dpa ligand. The diamagnetism of **3** has been established by ^{1}H−NMR spectroscopy,[17] and would be consistent with a W−W triple bond. However, the W−W distance in **3** is significantly longer than usually observed for triply bonded W_2^{6+} species (~2.4 Å),[25,26] and could suggest a bond order lower than 3 with strong antiferromagnetic coupling between the two W atoms. This bonding scheme finds precedence in the diamagnetic compounds (^{t}BuO)$_4$W$_2$(μ-PPh$_2$)$_2$ (d(W−W) = 2.59 Å)[27] and (Me$_2$N)$_4$W$_2$(μ-PCy$_2$)$_2$ (d(W−W) = 2.57 Å).[28]

Electrochemistry and Spectroscopy. The significantly higher solubilities of species **1BPh$_4$** and **2BPh$_4$** as compared to their quadruply bonded parents made it possible to investigate their redox properties by means of cyclic voltammetry (CV) (Figure 4 and 5). In both CVs we observe a reversible $M_2^{4+/5+}$ redox couple at −1193 mV for **1BPh$_4$** and at −832 mV for **2BPh$_4$** (potentials are referenced versus the ferrocene/ferrocenium redox couple). Interestingly, the $MoW^{4+/5+}$ couple in the recently published heterodimetallic compound $MoW(dpa)_4$[14] appears at a potential that lies between those reported here (−1043 mV). Compounds **1BPh$_4$** and **2BPh$_4$** experience a second oxidation at −578 mV and −44 mV, respectively, which is assigned to the $M_2^{5+/6+}$ oxidation. This electron transfer appears to be quasi-reversible for **1BPh$_4$** (but not for **2BPh$_4$**) depending on the potential range.

To interrogate the electronic structure of **1BPh$_4$** and **2BPh$_4$** further, X-band EPR spectra of CH_2Cl_2 solutions of these compounds were measured at room temperature (Figure 6). The spectra were simulated assuming complete delocalization of the single electron over both metal atoms and taking into account the natural abundance of 14.31% for isotope ^{183}W (I = 1/2) for **1BPh$_4$** and a combined abundancy of 25.47% for isotopes ^{95}Mo and ^{97}Mo (I = 5/2) in the case of **2BPh$_4$**. Compounds **1BPh$_4$** and **2BPh$_4$** display isotropic signals with g_{iso} = 1.863 (A_{iso} = 95 MHz) and g_{iso} = 1.951 (A_{iso} = 56 MHz), repectively. The g-values are very similar to those observed for [W$_2$(O$_2$C^{t}Bu)$_4$)][PF$_6$] (g_{iso} = 1.814, A_{iso} = 51 G) and [Mo$_2$(O$_2$C^{t}Bu)$_4$)][PF$_6$] (g_{iso} = 1.941, A_{iso} = 27 G),[29,30] and the fact that they are both lower than the free-electron g value agrees with the expectation that the compounds have a less than half-filled valence d shell.

Upon $M_2^{4+/5+}$ oxidation characteristic changes in the electronic absorption spectra are expected. The $^1(\delta\rightarrow\delta^*)$ transition in quadruply bonded compounds is often very weak and obscured by stronger charge-transfer bands, as in the case of **1** and **2** (Figure 7). However, the $^2(\delta\rightarrow\delta^*)$ transitions in M_2^{5+} compounds is commonly encoun-

(22) Cotton, F. A.; Daniels, L. M.; Murillo, C. A.; Zhou, H.-C. *Inorg. Chim. Acta* **2000**, *305*, 69–74.
(23) Berry, J. F.; Cotton, F. A.; Murillo, C. A. *Inorg. Chim. Acta* **2004**, *357*, 3847–3853.
(24) Müller-Buschbaum, K.; Quitmann, C. C. *Inorg. Chem.* **2006**, *45*, 2678–2687.
(25) Chisholm, M. H. *Acc. Chem. Res.* **1990**, *23*, 419–425.
(26) Manke, D. R.; Loh, Z.-H.; Nocera, D. G. *Inorg. Chem.* **2004**, *43*, 3618–3624.
(27) Buhro, W. E.; Chisholm, M. H.; Folting, K.; Eichhorn, B. W.; Huffman, J. C. *J. Chem. Soc, Chem. Commun.* **1987**, 845–847.
(28) Buhro, W. E.; Chisholm, M. H.; Folting, K.; Huffman, J. C.; Martin, J. D.; Streib, W. E. *J. Am. Chem. Soc.* **1988**, *110*, 6563–6565.
(29) Chisholm, M. H.; D'Acchioli, J. S.; Pate, B. D.; Patmore, N. J.; Dalal, N. S.; Zipse, D. J. *Inorg. Chem.* **2005**, *44*, 1061–1067.
(30) Cotton, F. A.; Daniels, L. M.; Hillard, E. A.; Murillo, C. A. *Inorg. Chem.* **2002**, *41*, 1639–1644.

Table 3. Selected Structural Parameters for the Ditungsten Compounds **1** and **1BPh$_4$**

1		**1BPh$_4$** ($C2/c$)		**1BPH$_4$** ($P2_1$)	
direction angle, deg	W···N$_{py}$(l), Å	direction angle, deg	W···N$_{py}$(l), Å	direction angle, deg	W···N$_{py}$(l), Å
12.9(5)	2.775(5)	29.0(3)	2.861(3)	27.5(3)	2.797(3)
12.9(5)	2.775(5)	29.0(3)	2.861(3)	29.3(3)	2.780(3)
40.5(5)	3.109(5)	9.9(3)	2.713(3)	30.0(3)	2.998(3)
40.5(5)	3.109(5)	9.9(3)	2.713(3)	13.7(3)	2.619(3)
∑ **106.8[5]**	**11.768[5]**	**77.8[3]**	**11.148[3]**	**100.5[3]**	**11.194[3]**

Table 4. Selected Structural Parameters for the Dimolybdenum Compounds **2** and **2BPh$_4$**

2		**2BPh$_4$** ($C2/c$)		**2BPH$_4$** ($P2_1$)	
direction angle, deg	Mo···N$_{py}$(l), Å	direction angle, deg	Mo···N$_{py}$(l), Å	direction angle, deg	Mo···N$_{py}$(l), Å
11.6(5)	2.786(5)	28.6(2)	2.868(2)	29.9(2)	2.808(2)
11.6(5)	2.786(5)	28.6(2)	2.868(2)	27.7(2)	2.815(2)
40.5(4)	3.155(4)	9.9(2)	2.720(2)	12.9(2)	2.630(2)
40.5(4)	3.155(4)	9.9(2)	2.720(2)	30.3(2)	3.029(2)
∑ **104.2[5]**	**11.882[5]**	**77.0[2]**	**11.176[2]**	**100.8[2]**	**11.282[2]**

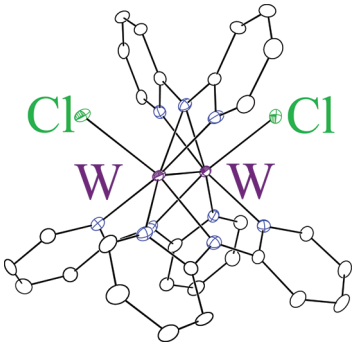

Figure 3. Molecular structure of $[W_2(dpa)_3Cl_2]^+$ from **3** with displacement ellipsoids drawn at the 30% probability level. Hydrogen atoms and the BPh_4^- counterion have been omitted for clarity.

Table 5. Selected Interatomic Distances in the $[W_2(dpa)_3Cl_2]^+$ Cation of **3** in **3·2CH$_2$Cl$_2$**

X	d(W1−X), Å	X	d(W2−X), Å
W2	2.5348(4)		
Cl	2.445(1)	Cl	2.407(2)
N1	2.184(5)	N3	2.186(4)
N2	2.136(5)	N2	2.128(5)
N4	2.211(5)	N9	2.190(5)
N5	2.107(4)	N8	2.095(5)
N7	2.151(5)	N6	2.152(4)

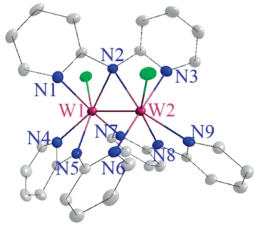

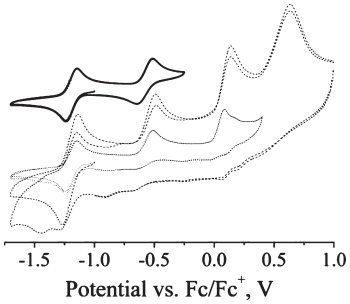

Figure 4. CV of **1BPh$_4$** in CH_2Cl_2 at several potential ranges.

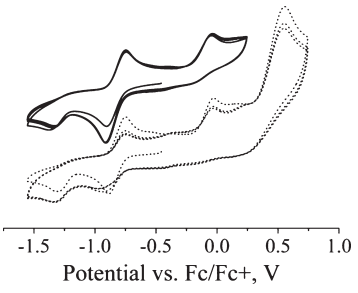

Figure 5. CV of **2BPh$_4$** in CH_2Cl_2 at several potential ranges.

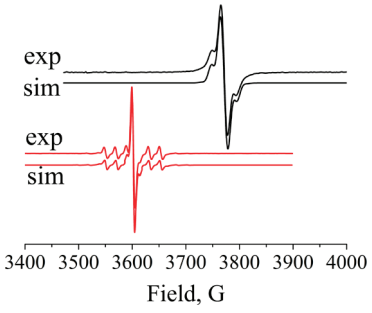

Figure 6. Experimental and simulated EPR spectra of solutions of **1BPh$_4$** (black) and **2BPh$_4$** (red) in CH_2Cl_2 measured at room temperature.

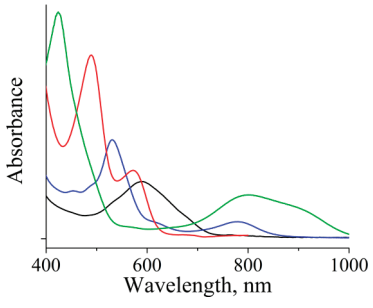

Figure 7. Electronic absorption spectra of solutions of **1** (black), **1BPh$_4$** (blue), **2** (red), and **2BPh$_4$** (green) in CH_2Cl_2 measured at room temperature.

tered at lower energy.[31] For CH_2Cl_2 solutions of **1BPh$_4$** and **2BPh$_4$** we observe bands at 781 and 801 nm, which we assign to the $^2(\delta\rightarrow\delta^*)$ transitions, and which are slightly lower in energy than the $^2(\delta\rightarrow\delta^*)$ transition reported for $M_2(O_2C^tBu)_4^+$ species (760 nm).[29]

Summary. In summary, the quadruply bonded compound **1** may be prepared directly from $W(CO)_6$ and dpaH in refluxing naphthalene. This is a remarkable observation, since preparation of related $W_2(N,N)_4$ compounds is usually quite involved. The choice of solvent for the reaction is critical, as we found that using 1,2-dichlorobenzene furnishes the cationic binuclear W(III) species **3**.

The W_2^{4+} unit in **1** is protected against axial coordination by the pendant pyridine rings of the dpa ligand. We therefore prepared the one-electron oxidized species **1BPh$_4$** and its molybdenum analogue **2BPh$_4$**, in which the M_2^{5+} units retained their primary coordination sphere. As a possible result of this encapsulation we found in **2BPh$_4$** the shortest Mo−Mo distance for Mo_2^{5+} compounds with bridging (N,N) donor ligands. Structural and spectroscopic evidence supports the M_2^{5+} assignment of these complexes with an unpaired electron in the M−M δ orbital and an overall M−M bond order of 3.5.

(31) Hopkins, M. D.; Gray, H. B. *Polyhedron* **1987**, *6*, 705–714.

Acknowledgment. We thank the National Science Foundation for support under CHE-0745500 and CHE-0741901 (Bruker EleXsys EPR) and CHE-9208463 (Bruker AC-300). We thank Ilia Guzei for assistance in the refinement of the crystal structure of **4**.

Note Added after ASAP Publication. This article was released ASAP on November 18, 2009, with footnote 30 missing. The correct version was posted on November 19, 2009.

Supporting Information Available: Additional information as noted in the text. This material is available free of charge via the Internet at http://pubs.acs.org.